J. COMBIN. MATH. COMBIN. COMPUT. 127a (2025) 9425--9544

Journal of Combinatorial Mathematics
and Combinatorial Computing
www.combinatorialpress.com/jcmcc

Research on fuzzy logic-based virtual power plant market trading model under decentralized trading mechanism

Jinqing Luo[1,✉], Shaohua Lin[1], Feng Qian[1], Kang'an Shu[1], Liu Yang[1], Qing Chen[1]

[1] *Guangdong Power Exchange Center Co., Ltd., Guangzhou, Guangdong, 510600, China*

ABSTRACT

With the promulgation of relevant policies, virtual power plant market transactions are facing major adjustments, in order to promote the smooth entry of virtual power plants into market-oriented transactions and improve the economic benefits of virtual power plants, this paper proposes a virtual power plant market transaction model. The traditional virtual power plant resources are mathematically modeled, blockchain technology is introduced to build a decentralized trading framework, and fuzzy neural networks are combined to predict the power load of the virtual power plant. Then the decision-making model of virtual power plant participation in spot market trading is constructed by using two-stage stochastic planning theory with the goal of maximizing expected return. The results show that the prediction effect of the fuzzy logic-based virtual power plant market trading model is 2.925% higher than that of the traditional BP algorithm model, and its accuracy and stability are significantly improved. In addition, the distributed energy storage aggregated by the virtual power plant as well as the dynamic demand response rate is fast, the regulation is flexible, the short-time power throughput capability is strong, and it can accurately track the FM instructions. The cumulative FM capacity and FM mileage provided by the virtual power plant account for 84% and 99% of the total FM capacity demand in the system, respectively, making it highly competitive in the FM market. And under the premise of balancing riskiness and profitability, the bidding scheme of virtual power plant derived in this paper is more effective.

Keywords: Virtual Power Plant, Blockchain Technology, Decentralized Transaction Mechanism, Stochastic Planning Theory, Fuzzy Neural Network Models

1. Introduction

With the continuous development of the energy market and technological progress, virtual power plant has gradually become a hot field of research at home and abroad. Virtual power plant is a system of centralized management and operation of distributed power supply and energy storage equipment,

✉ Corresponding author.
E-mail address: gdpxcps@126.com (J. Luo).

Received 25 March 2024; Revised 05 June 2024; Accepted 15 December 2024; Published Online 15 April 2025.
DOI: 10.61091/jcmcc127a-525

which integrates scattered energy resources through advanced software technology and communication technology [1-4], forming a unified power supply unit. In this context, the importance of the virtual power plant trading mechanism as an important bridge connecting the virtual power plant and the market is becoming more and more prominent [5-7].

The virtual power plant trading mechanism refers to the trading rules and processes of virtual power plants participating in the electricity market. Its core lies in the market-based means to achieve the balance of power and maximize the benefits between the virtual power plant and the power grid, users [8-9]. Virtual power plant trading mechanism includes the following aspects: market access mechanism is the first part of the virtual power plant to participate in the market. Virtual power plants must meet certain standards and conditions, after certification before trading in the electricity market [10-12]. Bidding and offer mechanism: virtual power plant based on their own power generation costs, market supply and demand and other factors, pricing and offer of power products. This link is the key for virtual power plants to gain revenue in the market. Power scheduling and transaction execution mechanism: after trading in the power market [13-16], the virtual power plant needs to carry out power scheduling and transaction execution according to the market demand and its own resources. This link needs to ensure the stability and reliability of power supply [17-18].

In this paper, we first study the framework of virtual power plant participation in electricity market trading, model the internal aggregated distributed resources in a refined way, and then construct the optimization model of virtual power plant (VPP) bidding with decentralized trading mechanism participation. For the scenario of multiple VPPs coexisting in the region, a joint FM decentralized trading mechanism based on blockchain technology is designed, which is responsible for the access and authorization of all shared energy storage nodes and thermal power unit nodes in the FM trading channel. Afterwards, a fuzzy neural network that combines the advantages of both fuzzy logic control and artificial neural network is used for short-term power load forecasting, which in turn improves the forecasting accuracy of the model. And in the results and analysis section, the effectiveness of the application of the virtual power plant market trading model is evaluated using a two-stage stochastic planning theory approach.

2. Fuzzy logic-based trading model construction for virtual power plant market

2.1. Modeling of virtual power plant resources

2.1.1. Overview of the virtual power plant:

1) Concept of Virtual Power Plant. The concept of virtual power plant (VPP) [19] is a flexible virtual cooperative relationship between independent market players that allows them to provide efficient power services to electricity consumers without having to own the corresponding assets and technologies. It can be summarized as the following: integrating some small distributed power sources to form a power plant-like structure, whose overall operational characteristics on the grid can be obtained by the aggregation of the characteristics of each distributed power source; integrating traditional power plants, distributed power sources, controllable loads, and energy storage resources in a certain area, and introducing a centralized control center for management to participate in the operation of the grid as a whole; and serving as a demand-side response method through a variety of demand-side measures to achieve the same effect as building an actual power plant.

2) Operation and control structure of virtual power plant. Virtual power plant, as the main body of multi-distributed resources integration, can not change the specific geographic location, equipment parameters and grid connection of distributed resources, but through advanced information and communication technology and control means to realize the distributed resources in the physical not directly connected to the role of the external coordination and unity of the flexible mode of operation.

At present, for different types of virtual power plants, mainly including centralized control, decentralized control and fully decentralized control of three control architectures.

Under the centralized control architecture, the VPP control center masters the parameters and operation information of all distributed resources it represents, and can formulate internal scheduling plans according to the overall goals of the VPP, and achieves complete control of each distributed resource through instant and efficient communication.

The decentralized control architecture breaks down the control center into two layers through hierarchical logic, where each lower control center is responsible for the management and control of several distributed resources, while the upper control center needs to break down the goals or tasks to the lower control center and receive the information feedback from the lower control center.

The fully decentralized control architecture divides the distributed resources in the virtual power plant into several communicating and intelligently autonomous subsystems without the role of a centralized control center. Each subsystem exchanges operational information and parameters, makes independent decisions, and gives operational control commands to the distributed resources it represents.

2.1.2. Modeling of virtual power plant resources:

1) Wind power generation unit. As an important distributed power source for virtual power plant aggregation, in-depth study of the output characteristics of the wind power unit is of great significance for improving the utilization rate of wind energy and the revenue of the virtual power plant. Many scholars have studied the wind speed simulation model, which is commonly used is the two-parameter Weibull distribution model [20], the wind speed is fitted by the scale parameter c and the shape parameter k, and the expression and its probability density function are shown below:

$$\begin{cases} v = \left| c(-\ln U) \right|^{\frac{1}{k}} \\ f(v) = \dfrac{k}{c}\left(\dfrac{v}{c}\right)^{k-1} \exp\left[-\left(\dfrac{v}{c}\right)^{k} \right] \end{cases} \tag{1}$$

where: U is a random variable obeying uniform distribution in the value range 0-1.

After having the wind speed data of a certain region, parameters c and k can be calculated according to the following formula based on the average wind speed μ and standard deviation σ of the region in a certain period of time:

$$k = \left(\frac{\sigma}{\mu}\right)^{1.086} \tag{2}$$

$$c = \frac{\mu}{\Gamma\left(1 + \frac{1}{k}\right)} \tag{3}$$

where: $\Gamma(x)$ denotes the Gamma function.

There exists a cut-in wind speed v_{in} for the wind turbine, when the actual wind speed $v < v_{in}$, the wind turbine output $P^{w} = 0$ before reaching the rated wind speed v_e of the unit, P^{W} with a v linear increase until it reaches the rated value $P_{ò}^{w}$ and then no longer changes, continuing to $P_{ò}^{w}$ output; when the wind speed is greater than the cut-out wind speed v_{ou}, in order to protect the fan blade will not be damaged due to the over-speed, at this time the wind turbine will be withdrawn from the operation. For the wind turbine output and wind speed of the relationship between the formula is as follows:

$$P^W = \begin{cases} 0 & v < v_{in} \\ \dfrac{v - v_{in}}{v_e - v_{in}} \cdot P_e^W & v_{in} \le v < v_e \\ P_e^W & v_e \le v < v_{out} \\ 0 & v > v_{out} \end{cases} \tag{4}$$

Wind turbines are determined by objective conditions. In this paper, the virtual power plant aggregated distributed wind turbine will participate in the transaction as a market subject, VPP in the different time scales of the market to submit bidding plans and internal resources out of the power arrangements, are required to forecast the power of wind turbines, this paper assumes that the prediction error of the wind power out of the power obeys the mean value of 0, the variance of σ_w of the normal distribution as the formula is shown below:

$$0 \le P_i^w \le P_i^{W,pre} \tag{5}$$

$$P_i^{W,pre} = P_i^{W,act} + \Delta P_i^W \tag{6}$$

$$\Delta P_i^w \sim N(0, \sigma_w^2) \tag{7}$$

where P_i^w is the actual grid-connected power of the WTGs, which is controlled by VPP after the VPP aggregation regulation; $P_i^{W,prò}$ and $P_i^{W,acc}$ represent the predicted and actual maximum output power of the WTGs at the moment of t, respectively; and ΔP_t^w represents the deviation of the prediction of maximum output power of the WTGs at the moment of t.

(2) Photovoltaic power generation unit

The photovoltaic power generation unit converts the solar energy irradiated to the photovoltaic panel into electricity by capturing the solar energy in the form of direct current, and its output is closely related to the geographical environment, light intensity and other climatic conditions. It is generally believed that light intensity obeys a Beta distribution, and the probability density function is shown below:

$$f(\gamma) = \frac{\Gamma(\alpha+\beta)}{\Gamma(\alpha)+\Gamma(\beta)} \left(\frac{\gamma}{\gamma_{\max}}\right)^{a-1} \cdot \left(1 - \frac{\gamma}{\gamma_{\max}}\right)^{b-1} \tag{8}$$

where $\gamma, \gamma_{\max}$ represents light intensity and maximum light intensity, respectively; α, β are two parameters in the Beta distribution.

Parameters α and β can be based on the historical light intensity mean w and standard deviation σ of the region as follows:

$$\alpha = w\left[\frac{w(1-w)}{\sigma^2} - 1\right] \tag{9}$$

$$\beta = (1-w)\left[\frac{w(1-w)}{\sigma^2} - 1\right] \tag{10}$$

When the light intensity does not reach the rated value of the unit, the output power varies linearly with the light intensity, and after reaching the rated value of the unit, the output power maintains the maximum value and does not change any more. For PV power generation unit the relationship between output power and light intensity is as follows:

$$P^V = \begin{cases} P_e^V \dfrac{\gamma}{\gamma_e} & 0 \le \gamma \le \gamma_e \\ P_e^V & \gamma > \gamma_e \end{cases} \tag{11}$$

where γ_e is the rated light intensity of the PV unit; P_e^v is the rated power of the PV unit.

VPP needs to forecast the maximum output of PV units when submitting bidding plans to the market at different time scales and when arranging the output of internal resources, and the normal distribution with a variance of σ_v is shown below:

$$0 \le P_i^V \le P_i^{V,pre} \tag{12}$$

$$P_i^{V,pre} = P_i^{V,act} + \Delta P_i^V \tag{13}$$

$$\Delta P_i^V - N(0, \sigma_V^2) \tag{14}$$

where p_i^v is the actual grid-connected power of the PV unit, which is controlled by the VPP after the VPP aggregation regulation; $P_i^{V,p\kappa}$ and $P_i^{V,act}$ represent the predicted and actual values of the maximum output power of the PV unit at the moment of 1, respectively: ΔP_i^V represents the deviation of the prediction of the maximum output power of the PV unit at the moment of t.

(3) Demand Response

Demand response refers to the behavior of an electricity consumer who responds to price signals or incentives to change the inherent pattern of electricity use.

In this paper, we consider that some of the internal loads represented by the VPP can participate in the incentive-based demand response, and we consider the leveling loads and interruptible loads respectively. Demand response loads can adjust their own load demand within a certain response capacity according to the incentives so as to provide equivalent output to the VPP, and two types of peak shaving demand response and valley filling demand response are set as follows:

$$P_t^{DR} = P_t^{dDR} - P_t^{\mu DR} (\forall t) \tag{15}$$

$$\begin{cases} u_t^{dDR} + u_t^{aDR} \le 1 \\ u_t^{dDR}, u_t^{aDR} \in \{0,1\} \end{cases} (\forall t) \tag{16}$$

where P_i^{DR} is the demand response at moment t; P_i^{dDR}, P_i^{aDR} is the load shedding response and load increasing response at moment t, respectively: u_i^{dDR}, u_i^{uDR} is the state variable of load shedding and load increasing demand response, respectively, and a value of 1 indicates that it is in that state.

The VPP pays a subsidy to the customer for the adjustment capacity provided by the load based on the peak shaving demand response unit price and the valley filling demand response unit price, respectively, which is the demand response cost to the VPP when the VPP performs the optimal scheduling plan as follows:

$$C^{DR} = \sum_t (K_{dDR} P_t^{dDR} + K_{aDR} P_t^{aDR}) \Delta t \tag{17}$$

where K_{aDR}, K_{uDR} is the subsidized unit price for load shedding demand response and load increasing demand response, respectively; P_i^{dDR}, P_i^{uDR} is the amount of response power for load shedding demand response and load increasing demand response, respectively, at moment t.

2.2. *Design of decentralized transaction architecture based on blockchain technology*

2.2.1. Alliance Chain Architecture Considering Access to Trading Entities. In this paper, we adopt the architecture of Hyperledger Fabric [21] to set up an authentication node (CA) in the blockchain network responsible for the access and authorization of all the shared energy storage nodes and thermal power unit nodes in the FM trading channel and issue unique digital signatures to the nodes on the chain. These shared energy storage nodes and thermal unit nodes are known as Peer (Peer) nodes.

2.2.2. Joint FM smart contract design. Smart contract realizes the synchronous circulation of information and value in the underlying framework through Turing's complete programmable function and the reading of real and trustworthy transaction information. Smart contract in Hyperledger Fabric is essentially a distributed transaction program on each peer node, which is automatically executed according to the transaction rules and strategies and updates the state of the ledger. At the end of the trading session, the thermal power unit and the shared energy storage that have reached a deal confirm the transaction with digital signatures respectively, and the smart contract validates and automatically completes the settlement of expenses and the transfer of the right to control the energy storage. The settlement contract on the thermal power unit node reads the transaction unit price and transaction volume, clears the transaction fee, and transfers the leasing fee from the account of the thermal power unit to the account of the shared energy storage.

The energy storage devices are all accessed in the blockchain network through IoT technology and have unique resource locators and corresponding access control policies, which determine that nodes with specific addresses can only control the charging and discharging power of the energy storage. After the verification fee reaches the account, the resource sharing contract on the energy storage node adds the address of the thermal power unit node to the accessible address by modifying the access control policy and automatically expires at the end of the leasing time, so as to realize the time-limited transfer of the energy storage control authority. At the end of the leasing time, the smart contract updates the transaction credit score of each node based on the behavior of the thermal power unit and the energy storage node. The credit score is based on whether the energy storage equipment has exceeded the agreed state of charge (SoC) limit under the control of the thermal power unit node, and whether the shared energy storage node has privately controlled the charging and discharging power of the energy storage.

2.2.3. Consensus Algorithm for Matching Degree. The Hyperledger Fabric architecture optimizes the design of the data uploading process: before the data consensus, the transaction information will be sent to the endorsing node for transaction simulation and attach the digital signature of the endorsing node; the peer nodes will verify whether the transactions in the block have the signatures of the endorsing node as well as whether they have been modified during the consensus process before depositing them into the block, and the tampered transaction data will be marked as invalid Data. This design effectively avoids the situation of consensus nodes committing evils, so the crash-tolerant class of consensus algorithms, which only considers faulty nodes but is more efficient, can be chosen.

The consensus flow that takes into account the credit matching degree of shared energy storage and thermal power units is shown in Fig. 1. The client first sends the market transaction information to the endorsing node for transaction simulation and attaches a digital signature, which is then returned to the client by the endorsing node. The client sends the endorsed transaction data to the master node, which sends it to the slave nodes through the heartbeat mechanism. When more than half of the sorting nodes confirm the acceptance of the transaction data, the sorting service is considered to have reached a consensus. Then all the sorting nodes pack the transaction information into an ordered block and send it to the peer node with bookkeeping authority, and the peer node verifies the digital signature and whether the data has been tampered with and then uploads the data onto the chain.

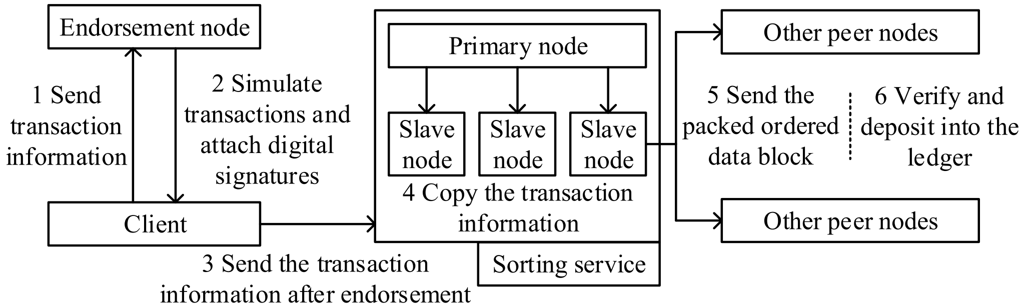

Fig. 1. Consensus flow chart for energy storage and credit matching

2.2.4. Classified storage of transaction data. When transaction data is stored on the blockchain, if every node on the blockchain stores all the transaction data, it will lead to problems such as data privacy leakage, insufficient synchronization performance of the blockchain and storage redundancy. With the drastic increase of transaction volume and data volume in the future, the development trend of blockchain nodes from full storage to partial storage will become the development trend. In this paper, the data is divided into 2 categories, public data and private data, according to the privacy of the data, and the distributed ledger on each node is divided into public ledger and private ledger through the aggregation technology to realize the data categorization and storage. Among them, the public data is the transaction information that is publicized during the transaction process, including the demand of thermal power units for energy storage and the credit score of the transaction, the sold capacity of shared energy storage and other attributes. This information needs to be backed up and stored by all nodes, and all nodes have query privileges. The private data includes the transaction records and offer information of each node, and the real content of the private data is only stored in the private ledger of the shared energy storage and the thermal power units that have reached a deal, while its hash value is stored in the public ledger of all nodes on the chain, and only the two parties to the deal can query the real content of the private data.

In the transaction execution phase, the smart contract on the nodes of both parties to the transaction reads the content of the private data and carries out the account payment and control transfer. If there is a subsequent dispute between the two parties, they can choose to share the real content of private data to a third party node for hash verification. Private data on the chain also needs to be verified by the sorting node, but the sorting node can only query the encrypted hash value of the data and pack it into an ordered block to be sent to other nodes to be stored in the public ledger.

2.3. Construction of Short-term Electricity Load Forecasting Network Models

2.3.1. Sample load data collection and processing:

1) Handling of abnormal data. When collecting samples, there will be anomalous or pseudo-data in the collected data due to various reasons, and these anomalous data will have a large negative impact on the forecast results. For a specific area, the daily maximum load and daily minimum load of two adjacent days generally do not differ too much, and there is a certain limit to the load change at adjacent moments on the same day, and the change is also somewhat regular. Using these characteristics, it is possible to find abnormal data and eliminate them.

The same day of the two adjacent moments of the load change will not show explosive changes, so we can set a threshold, as long as the absolute error of the two moments before and after the threshold does not exceed the data is not considered abnormal data: otherwise, it is abnormal data.

That is, if:

$$\left|S(d,t)-S(d,t-1)\right|>\theta(t) \tag{18}$$

Then:

Where: $S(d,t)$ is the value of the load at the t moment of the d nd day, and $\theta(t)$ is the threshold value.

Power load has a period of 24 hours of periodicity, so the load of the same moment of two adjacent days will not show explosive changes, but has a certain similarity, the change should also be within a certain range. If it is out of this range, it is abnormal data.

That is, if:

$$\left|S(d,t)-M(t)\right|>\gamma(t) \tag{20}$$

Then:

$$S(d,t)=M(t)+\gamma(t),\text{if } S(d,t)>M(t) \tag{21}$$

$$S(d,t)=M(t)-\gamma(t),\text{ if } S(d,t)<M(t) \tag{22}$$

where: $M(t)$ is the load average of the sample load data for recent days t moments, and $\gamma(t)$ is the threshold value.

2) Handling of missing data. If there is missing data for a particular day, the data for that day is said to be missing data. The usual method used is to repair the data with the same date type adjacent before and after.

Namely:

$$S(d,t)=\alpha_1 S(d+1,t)+\alpha_2 S(d-1,t) \tag{23}$$

where: α_1,α_2 is the weight.

3) Normalization of sample load data. Because the fuzzy neural network learning training sample load data has a limited range, so in order to accelerate the convergence of the network and improve the prediction accuracy, the samples should be normalized or standardized before training.

If the sample load data is to be converted to the range of (-1, 1), the formula is as follows:

$$y=\frac{x-\frac{1}{2}(x_{\max}+x_{\min})}{\frac{1}{2}(x_{\max}-x_{\min})} \tag{24}$$

where: x is the sample load value, $x_{\max}$ the sample load maximum value, and $x_{\min}$ the sample load minimum value.

To convert the sample load data to the range (0, 1), the formula is as follows:

$$y=\frac{x-x_{\min}}{x_{\max}-x_{\min}} \tag{25}$$

Different normalization ranges will directly affect the convergence speed and prediction accuracy of the network, and the range of the conversion should be compatible with the effective working interval of the activation function, and it is better that the conversion range is slightly smaller than the working interval of the activation function, so that the network model is more extrapolated.

Therefore, in this paper, the sample load data are converted to the range of (0.1, 0.9), and the formula used is as follows:

$$y=0.8*\frac{x-x_{\min}}{x_{\max}-x_{\min}}+0.1 \tag{26}$$

2.3.2. Fuzzification of influencing factors:

1) The fuzzy processing of humidity in order to improve the prediction accuracy and combined with the prediction of the temperature situation in the region, the temperature of the following fuzzy processing with five affiliation functions: in order to make the calculation convenient, and taking into account the type of affiliation function selection on the fuzzy impact is not large, so this paper selected trapezoidal and triangular affiliation function.

The trapezoidal distribution is used for the low-temperature affiliation sigmoid:

$$T=\begin{cases}0 & t\geq 10\\ \dfrac{10-t}{10} & 0<t<10\\ 1 & t\leq 0\end{cases} \tag{27}$$

A triangular distribution was used for the low and medium temperature affiliation functions:

$$T=\begin{cases}\dfrac{t-5}{10-5} & 5\leq t<10\\ \dfrac{15-t}{15-10} & 10\leq t\leq 15\\ 0 & t<5 \text{ or } t>15\end{cases} \tag{28}$$

A triangular distribution was used for the mesothermal affiliation function:

$$T=\begin{cases}\dfrac{t-10}{20-10} & 10\leq t<20\\ \dfrac{30-t}{30-20} & 20\leq t\leq 30\\ 0 & t<10 \text{ or } t>30\end{cases} \tag{29}$$

A triangular distribution was used for the medium and high temperature affiliation functions:

$$T=\begin{cases}\dfrac{t-25}{30-25} & 25\leq t<30\\ \dfrac{35-t}{35-30} & 30\leq t\leq 35\\ 0 & t<25 \text{ or } t>35\end{cases} \tag{30}$$

A trapezoidal distribution is used for the high temperature dependency function:

$$T=\begin{cases}1 & t\geq 40\\ \dfrac{t-30}{40-30} & 30<t<40\\ 0 & t\leq 30\end{cases} \tag{31}$$

According to the principle of maximum affiliation, the affiliation function and fuzzy set to which the maximum affiliation belongs can be known.

2) Fuzzy processing of weather. According to the year-round weather conditions in the forecast area, the fuzzy processing is carried out, and the results of the fuzzy processing of weather conditions are shown in Table 1.

Table 1. Fuzzy treatment of weather conditions

Serial number	Weather condition	Fuzzy value
1	Heavy snow	0.01
2	Medium snow	0.02
3	Small snow	0.03
4	Heavy rain	0.04
5	Medium rain	0.05
6	Small rain	0.06
7	Cloudy day	0.07
8	Cloudy	0.08
9	Sunny day	0.09

2.3.3. Design of fuzzy neural network models:

1) Design of the number of network nodes. The most common method to set the number of nodes in the hidden layer is the "trial and error method", i.e., the number of nodes in the hidden layer is set according to the empirical formula first, and then slowly increase, and select the number of nodes corresponding to the minimum error, which is the final number of nodes. Below are some common empirical formulas:

$$p = \sqrt{m+n} + a \tag{32}$$

$$p = \log 2 * p = \sqrt{mn} \tag{33}$$

where: p is the number of nodes in the hidden layer, m is the number of nodes in the input layer, n is the number of nodes in the output layer and a is a constant between 1 and 10.

2) Network transfer function set juice. According to the intrinsic law of power load and the need for prediction, this paper selects the tangent tansig function as the hidden layer transfer function and the logsig function as the output layer transfer function. Its formula is as follows:

$$\tan sig(n) = \frac{2}{1+\exp(-2n)} - 1 \tag{34}$$

$$\log sig(n) = \frac{1}{1+\exp(-n)} \tag{35}$$

3) Design of network initial weights. The initialization of the network weights has a great impact on the training time, and choosing the appropriate initial weights can greatly shorten the network training time. There are usually two methods: one is to set the initial weights small enough: the other is to set an equal number of initial weights as +1 and -1. No matter which method is used, the following two principles should be observed:

Setting the maximum value of the initial weights to 1 is a reasonable choice;

The range of values of the initial weights is related to the transfer function. When the transfer function is a tangent tansig function, the range of values of the initial weights is (-1, 1); when the transfer function is a logsig function, the range of values of the initial weights is (0, 1).

4) Setting up the learning parameters of the network. The learning rate determines the amount of change in the weights of the network after each learning training. If the learning rate is too small, although it can ensure the convergence of the network, the convergence speed will be very slow, which greatly increases the training time; if the learning rate is too large, the network system may lead to

oscillations or dispersion due to too fast learning speed, which will cause the system to collapse. Moreover, when the learning rate increases to a certain extent, its effect on the convergence speed, training time and number of times of the network does not change significantly and does not decrease as the learning rate continues to increase. Out of consideration of the convergence of the network, a smaller learning rate is generally chosen, with values ranging from 0 to 1.

The momentum factor is the inertial momentum hall term, which plays a very important role in regulation. The network may fall into a local minimum during training, which means that the single training error is basically unchanged, so its return value on the adjustment of the weights is very small, but the total error is greater than the total error set by the training. At this point, the addition of a momentum factor helps to feed back the error value so that the neuron's weights oscillate again. The momentum minima reduces the likelihood of an oscillatory trend during training, thus effectively inhibiting the network from falling into a local minimum, improving convergence, and finding a better solution. However, the disadvantage of this method is also obvious, it has a high requirement on the initial weights. A large number of practices have proved that the network training effect is better when the momentum factor obtains larger than the learning rate. Therefore the momentum factor is taken as 0.1 in this paper.

3. Results and analysis of whole-day power load forecasts

In this paper, 96 points of daily load data and 24 points of meteorological data are selected as the training samples of the network in the load system of a region in X city from October 1, 2023 to November 14, 2023, and the 24-point load prediction is carried out with the traditional BP algorithm and this paper's algorithm on December 15 and December 19, 2023 respectively with the trained network. The results of the whole-point load prediction on December 15 are shown in Table 2. 15 whole point load prediction results are shown in Table 2. The prediction results show that the average absolute error, the maximum relative error and the minimum relative error of the traditional BP algorithm model prediction are 4.02%, 6.96% and -1.88%, respectively; while the values of these three indexes of this paper's algorithm model prediction are 1.095%, 3.63% and 0.17%, respectively. Through the prediction comparison and error analysis, the load prediction results are better. All the results obtained by the prediction model in this paper are significantly better than the traditional BP algorithm, so the algorithm in this paper greatly improves the accuracy and stability of load forecasting, which is crucial for short-term load forecasting.

Table 2. The results of the load forecast on December 15

Time (hour)	Actual value(MW)	Traditional bp algorithm		This algorithm	
		Predictive value(MW)	Error (%)	(MW)	Error (%)
0:00	746.087	761.655	-4.07	741.958	1.05
1:00	752.793	787.374	-5.08	747.724	0.6
2:00	744.999	728.958	-2.16	752.185	-0.71
3:00	673.392	609.023	4.09	668.356	0.85
4:00	702.270	735.683	-3.94	691.983	0.67
5:00	749.478	723.522	4.04	742.819	1.18
6:00	763.108	738.914	3.98	755.176	0.81
7:00	742.484	759.501	3.64	741.265	0.17
8:00	852.969	821.119	3.92	850.880	1.07
9:00	846.733	798.893	3.96	857.461	-0.61
10:00	733.138	777.972	-3.84	749.277	0.72

11:00	791.244	661.176	4.12	785.823	1.68
12:00	789.129	732.915	4.13	785.851	0.82
13:00	693.611	664.651	3.14	682.708	2.62
14:00	785.733	756.212	4.09	780.095	0.76
15:00	687.736	659.114	3.96	689.769	-0.66
16:00	801.968	861.268	3.95	746.648	3.63
17:00	680.969	702.289	-1.88	672.132	-0.86
18:00	1121.825	1096.744	3.86	1112.899	0.83
19:00	1256.740	1158.491	4.19	1253.535	0.54
20:00	1252.170	1228.666	6.96	1260.790	-1.95
21:00	1235.937	1186.860	4.26	1213.798	1.85
22:00	1051.204	1045.617	4.11	1048.478	0.97
23:00	909.394	855.345	5.04	908.585	0.67

4. Two-stage decision-making model for virtual power plant participation in spot market transactions

4.1. Virtual power plant uncertainty analysis

The virtual power plant contains distributed power sources, which will encounter various uncertainties in operation, and these uncertainties need to be quantified in order to increase the universality of the model. When declaring power to each market, the virtual power plant will face the uncertainty of the electricity price of each trading moment in the day-ahead market and the real-time market, which will have a significant impact on its operating income, so the uncertainty of the electricity price should be analyzed and processed when constructing the decision-making model. Light intensity and wind speed variations can be approximated as stochastic variants consistent with Beta distribution [22] and Weibull distribution, which also have significant uncertainties. Due to the small size of the customer load under consideration and the small volatility of the load measurements, this paper does not take into account the uncertainty in the customer load and uses the typical daily customer load forecast demand curve as the actual customer load curve.

4.2. Two-Stage Stochastic Programming Theory Analytical Approach

1) Two-stage stochastic planning theory. Stochastic programming theory is a kind of uncertain optimization theory, developed from linear programming, mainly used to solve the objective function and constraints contain uncertain coefficients in the mathematical problems, in order to help decision makers in the uncertain environment to make reasonable decisions. With the deepening of the research and the needs of practical problems, two-stage stochastic programming theory to solve the need to make decisions in two different phases of the problem, its general form can be expressed as:

$$\begin{cases} max\, c^T x + E[max_{y_a}\, q_\omega^T y_\omega] \\ s.t: \\ \underline{b} \le Ax \le \overline{b} \\ \underline{h}_\omega \le T_\omega x + W_\omega y_\omega \le \overline{h}_\omega, \forall \omega \\ x \ge 0, y_\omega \ge 0, \forall \omega \end{cases} \tag{36}$$

where x and y_a are the first and second stage variables respectively, c^T is the coefficient of the objective equation of the first stage variable x, and q_ω^τ is the coefficient of the objective equation of the second stage variable y_ω; in the constraints, top and $\overline{b}$ are the upper and lower bounds of the constraints of the first stage variable respectively, and A is the constraints coefficients matrix of the first stage; h_ω and $\overline{h}_\omega$ are the upper and lower bounds of the constraints of the second stage variable, which need to be greater than zero in both stages, ω is the the set of scenarios, the above problem can be equivalently transformed into the following form according to the approach in the literature:

$$\begin{cases} \max_{x,y_a} c^T x + \sum_{\omega}^{\Omega} \rho_\omega q_\omega^T y_\omega \\ s.t: \\ \underline{b} \le Ax \le \overline{b} \\ \underline{h}_\omega \le T_\omega x + W_\omega y_\omega \le \overline{h}_\omega, \forall \omega \\ x \ge 0, y_\omega \ge 0, \forall \omega \end{cases} \tag{37}$$

In equations containing random variables that cannot be solved directly, the general idea of solving is to use the expected value to replace the random variables in the model, i.e., to turn the uncertainty problem into a deterministic problem and thus solve it, but when the expected value of the random variables is difficult to obtain directly, it is also possible to generate several different scenarios with the uncertainty of the random variables, and use scenario analysis to describe the uncertainty of the wind power and the PV output power.

2) Scenario analysis method. In stochastic planning, scenario analysis method is an effective method to deal with uncertainties. Scenario analysis generates a set of scenarios through certain data simulation methods, and transforms the optimization problem with uncertainties in the original equations into an optimization problem that seeks the expected value of multiple deterministic equations. Scenario set is a collection constructed based on time-ordered variables, for the combined output of wind power and photovoltaic in the following day t time period can be recorded as a scene q within the scenario set, and the corresponding weights are assigned to indicate the probability of the scene occurring on the following day, the collection composed of all the scenarios q that is, the scenario set, denoted by Q, or can be expressed as a scenario tree in the form of a structure, which can be divided into a general structure, sector structure and tree structure.

4.3. Stochastic Planning Decision Model for Virtual Power Plants

For the virtual power plant, its participation in spot market trading can be divided into two stages, the first stage is to make a day-ahead declaration decision in the case of unknown scenario of wind and solar power and electricity price, and the second stage is to make an imbalance adjustment plan for each time period of power by using the energy storage unit, distributed gas unit, and demand response resources under the real-time updating of the wind and solar power, and the profit of the virtual power plant can be divided into day-ahead market revenues, real-time market power regulation revenues (and possibly expenses), and after considering the uncertainty of wind-scenic output and tariffs, the objective function of its decision-making model will change to maximize the expected return that includes all scenarios, i.e.:

$$\hat{R}_{np} = \max \sum_{t=1}^{T} \sum_{s=1}^{M} \pi_{ss} \sum_{s=1}^{N_1} \gamma_s \sum_{s=1}^{N_2} \gamma_s \{R_{t,ss}^{Ds} + R_{t,s,v,s}^{Bt} - C_t^F - C_t^{sss} - C_t^B\} \tag{38}$$

$$\hat{R}_{np} = \max \sum_{s=1}^{M} \pi_{ss} R_{t,ss}^{Ds} + \max \sum_{t=1}^{T} \sum_{s=1}^{M} \pi_{ss} \sum_{s=1}^{N_1} \gamma_s \sum_{s=1}^{N_2} \gamma_s \{R_{t,s,ss}^{B} - C_t^F - C_t^{sss} - C_t^B\} \tag{39}$$

where ω, s and v are the set of scenarios for the joint tariff and the set of scenarios for the respective output of wind and solar, respectively, R_{ts}^{lo} and $R_{\tau,s,v,s}^{k}$ are the revenues gained by the virtual plant from participating in the day-ahead and real-time markets, respectively, and C_i^F, C_i^{iB} and

$C_i^{\kappa es}$ denote the operating cost of the distributed gas unit, the cost of applying incentive-type demand response to the users, and the charging and discharging cost of the energy storage battery, respectively.

1) Day-ahead Market Benefits. The virtual plant operator will submit day-ahead bids for power P_t^{Do} under each time slot on the following day, and after winning the bid, each unit will participate in the dispatch of power generation during actual operation. $\lambda_{7,a}^{\Omega a}$ denotes the price of each time slot in the day-ahead market phase under the joint scenario, and the total revenues from the virtual plant bids in the day-ahead market $R_{i,\infty}^{\mathrm{jo}}$ and day-ahead bids in the day-ahead market on the following day can be denoted as follows.

$$R_{i,s}^{Da} = \lambda_{\gamma,s}^{Da} P_i^{Da} \tag{40}$$

$$P_t^{Da} = W_t^{Da} + PV_t^{Da} - L_t \tag{41}$$

2) Real-time market gains. In the second stage, i.e., before the real-time market opens, the virtual plant operator will get the just updated wind and PV outputs, and at this time, the output curves will deviate from the bidding power in the previous day. In this paper, we use the energy storage battery, the distributed gas unit and the user-side demand response to track the change of the wind and PV outputs, and serve as a balancing unit to smooth out the deviation of their outputs:

$$P_{i,s,v,\omega}^{R} = W_{i,s,\omega} + PV_{i,v,\omega} + P_i^{essd,R} - P_i^{ess,Rt} - P_i^{Da} + G_i^{f} + IB_i \tag{42}$$

$W_{t,s,a}$ and $PV_{t,t,a}$ represent the updated wind power values before the real-time market opens, $G_i^{'}$ is the power value of the gas unit, and IB_i represents the value of the cut-off load on the customer side at the moment of t. The virtual power plant operator can offer the customer a certain amount of cash compensation so that the customer will reduce its own load at a certain moment out of economic reasons, and the operator can utilize this part of the cut-off load to participate in the real-time market trading as the power, and make profits from it. Profit. When $P_{t,y,\omega}^{8t} \geq 0$, it means that the actual output of the virtual power plant is higher than the declared output of the day before, then the virtual power plant can provide up-regulation standby service in the real-time market, and it will be sold at a price lower than the real-time market, when $P_{i,s,r,a}^{Rt} \leq 0$, it means that the actual output of the virtual power plant is lower than the declared output of the day before, then the virtual power plant needs to buy power at a price higher than the real-time market in the real-time market in order to satisfy the power requirement, and the profit or expense gained at the stage of real-time market is as follows The profit or expense obtained in this stage is:

$$R_{t,s,v,s}^{B} = (1-\theta)\lambda_{t,s}^{B}\Delta_{t,s,v,s}^{+} - (1+\theta)\lambda_{t,s}^{B}\Delta_{t,s,v,s}^{-} \tag{43}$$

$$P_{t,s,v,s}^{Br} = \Delta_{t,s,v,s}^{+} - \Delta_{t,s,s}^{-} \tag{44}$$

$$\Delta_{t,s,v,\omega}^{+} = max\{P_{t,s,v,\omega}^{Bt}, 0\} \tag{45}$$

$$\Delta_{t,s,v,\omega}^{-} = max\{-P_{t,s,v,\omega}^{Bt}, 0\} \tag{46}$$

where θ is a penalty factor indicating that the virtual power plant will have to sell power in the real-time market at a price lower than the real-time price and buy power at a price higher than the real-time price.
Distributed power output constraint:

$$0 \leq W_t^{Da} \leq W^{ma} \tag{47}$$

$$0 \leq PV_t^{Da} \leq PV^{ma} \tag{48}$$

Energy storage battery operation constraints:

$$\alpha_t^c P_t^{essc,min} \le P_t^{essc} \le \alpha_t^c P_t^{essc,max} \tag{49}$$

$$\alpha_t^d P_t^{\cos d,\min} \le P_t^{\cos d} \le \alpha_t^d P_t^{\cos d,\max} \tag{50}$$

$$E_t^{mas} \le E_t \le E_t^{\max} \tag{51}$$

$$\alpha_t^c + \alpha_t^d \le 1 \tag{52}$$

Gas unit operating constraints:

$$\mu_t^c G^{fins} \le G_t^f \le \mu_t^c G^{finss} \tag{53}$$

$$-\Delta G \le G_t^f - G_{t-1}^f \le \Delta G \tag{54}$$

Incentive-based demand response constraints:

$$0 \le IB_i \le \eta_i L_i \tag{55}$$

$$-\Delta IB^{mx} \le IB_t - IB_{t-1} \le \Delta IB^{mxx} \tag{56}$$

At this point, the construction of a two-stage stochastic planning model for virtual power plant participation in spot market trading is completed.

5. Analysis of the effectiveness of the application of the virtual power plant market trading model

5.1. Parameters of the algorithm

This paper takes VPP1 as an example for simulation, selects a 160MW wind farm as the wind power generation resource aggregated by the virtual power plant, generates the data of wind power generation under different scenarios according to the data of this wind farm in 2023, and utilizes the clustering algorithm to get the data of wind power output of this wind farm on a typical day, and sets the maximal fluctuation deviation as 10%. A 120MW photovoltaic power plant is selected as the photovoltaic power generation resource aggregated by the virtual power plant, and the data of photovoltaic power generation under different scenarios are generated according to the data of the photovoltaic power plant in 2023, and the power output data of the photovoltaic power plant on a typical day is also obtained by using the clustering algorithm, and the maximum fluctuation deviation is set to be 10%, and the predicted power curves of wind and light are shown in Fig. 2.

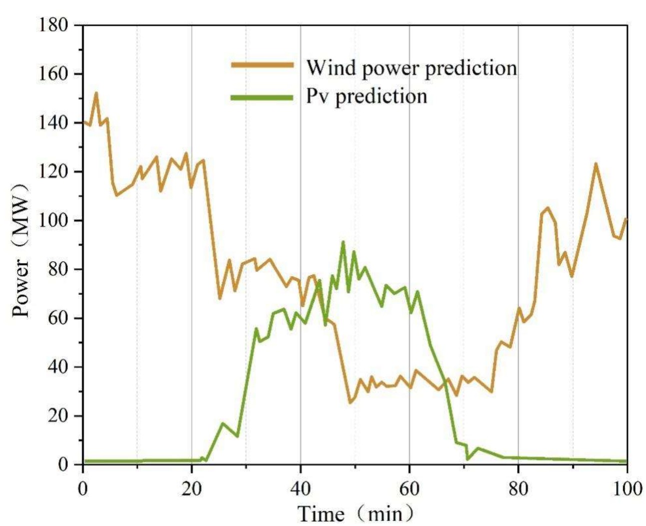

Fig. 2. The scenery forecast the output curve

Aggregate 510 interruptible loads to participate in the electric energy market transactions, and aggregate 510 levelizable loads to participate in the FM ancillary services market; the uncertainty parameter of the robust model is taken as $\Gamma^{wr} = 12, \Gamma^{pv} = 6$. The conventional generators use segmented offers in the electric energy market with a segment number of 10; the mileage-to-capacity ratio is 15. The system FM capacity demand is shown in Fig. 3.

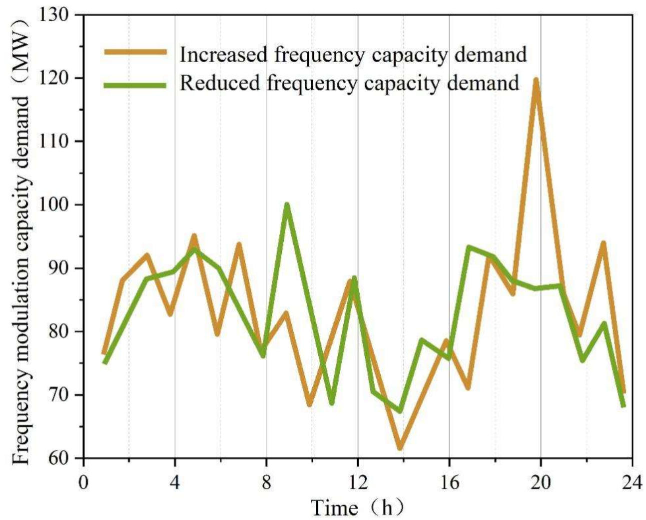

Fig. 3. System frequency modulation capacity demand

5.2. *Bids won in the electric energy-FM market*

The winning bids in the electric energy market are shown in Figure 4. In the electric energy market, traditional power producers always occupy the mainstay position, and the amount of electric energy borne by them during the daytime hours can be more than 25%, especially during the period of 11:00-13:00 to meet the demand for electric energy as high as 46.31-62.70%, which reflects the prevalence and importance of the traditional power producers in the provision of electric energy. However, it is clear that the virtual power plants win more bids in the energy market during the night hours, which is mainly due to the strong wind at night. It is worth noting that there are cases where virtual plants do not win the bidding, and there are cases where market participants with higher bids do not win the bidding when the load demand is relatively low, such as during the hours of 5:00, 8:00 and 9:00.

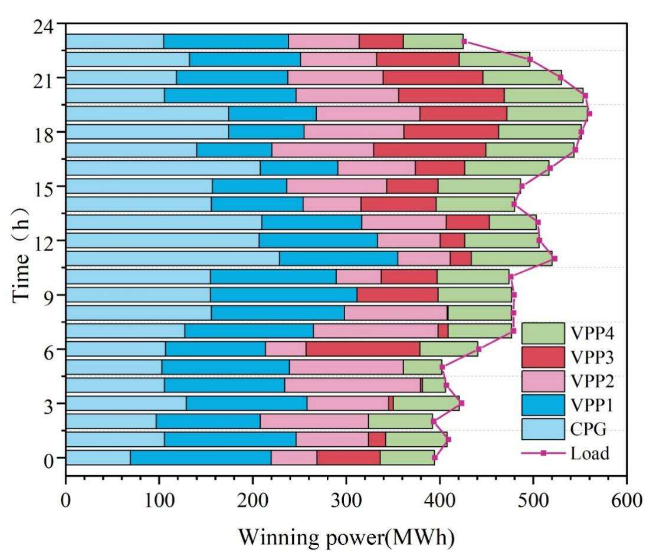

Fig. 4. Power quantity market bid

The winning bids in the FM ancillary services market are shown in Figure 5 (a indicates winning bids for FM capacity; b indicates winning bids for FM mileage). Compared with traditional generators, virtual power plants have taken up relatively more FM tasks in the FM market. The cumulative FM capacity provided by virtual power plants accounts for 84% of the total FM capacity requirement in the system, and the cumulative FM mileage accounts for 99% of the total FM mileage requirement in the system. This is because the mileage-to-capacity ratios of virtual power plants are typically larger than those of conventional generators, meaning that when providing the same amount of FM capacity, virtual power plants tend to be able to provide more FM miles compared to conventional generators. For FM signals, traditional power producers inevitably have the shortcomings of long response time, low unit ramp rate, delayed regulation, and inability to accurately track FM commands issued by the grid; whereas the distributed energy storage and dynamic demand response aggregated in the virtual power plant, with its fast response rate, flexible regulation, and strong short-term power throughput capability, can accurately track FM commands, and is a rare and high-quality FM resource. Therefore, virtual power plants can be prioritized to be called in the FM auxiliary service market. Meanwhile, it can be seen from the figure that among the virtual power plant market participants, VPP1 has a great advantage in providing FM capacity and FM mileage, indicating that the FM service provided by VPP1 has a fast response rate, short response time and good response accuracy.

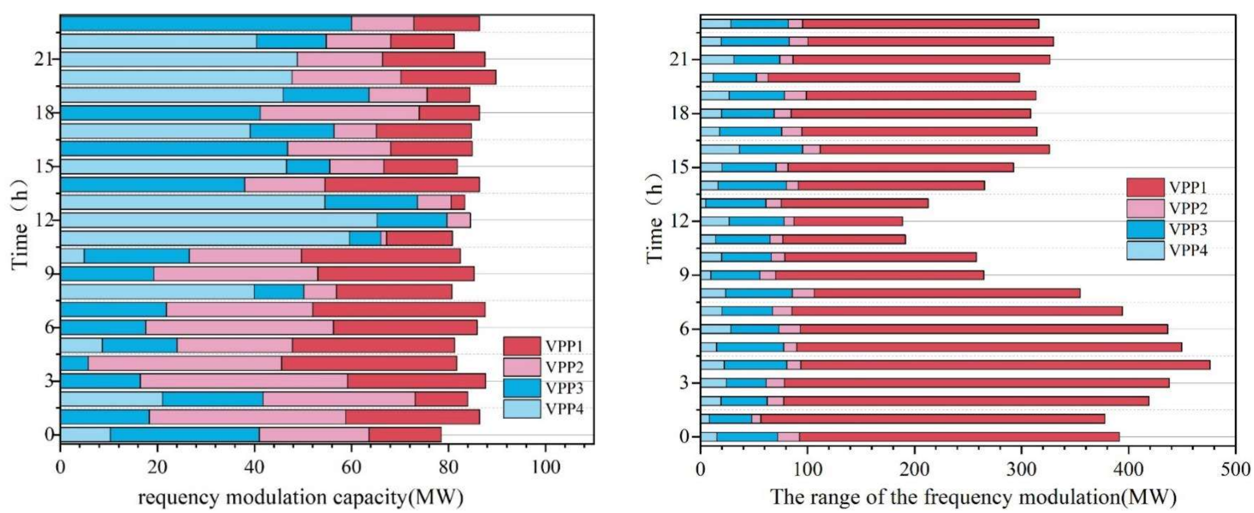

(a)Frequency modulation capacity winning situation (b)The winning of FM miles

Fig. 5. Frequency modulation auxiliary service market

5.3. Electric Energy-FM Market Clearance Prices

The electricity energy market clearing price is shown in Figure 6. It can be seen that the price of electricity in each time period is positively correlated with the load demand, and the trend of the clearing price is similar to the trend of the load demand, which is high during the daytime and slightly lower at night. This is because during the daytime, traditional power producers are mainly responsible for power generation, and their offer is based on the cost of power generation, thus showing a linear correlation between the offer and power generation; at night time, virtual power plants are the main power producers, and their relative offer is lower, resulting in lower clearing prices.

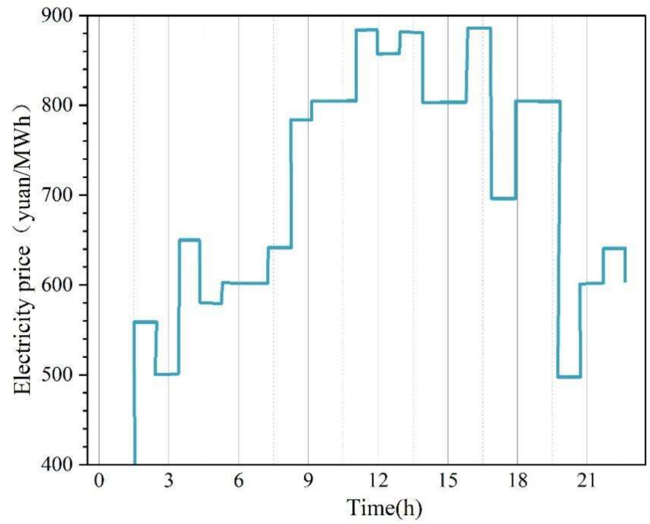

Fig. 6. The power quantity market clears the price

The clearing prices in the FM ancillary services market are shown in Figure 7 (a indicates FM capacity clearing prices; b indicates FM mileage clearing prices). It can be seen that the clearing price of FM capacity is similar to the trend of FM demand, for example, the demand for up FM capacity and the price of up FM capacity peak at 8:00-10:00 and 14:00-15:00, the demand for down FM capacity and the price of down FM capacity trough at 13:00-14:00, and the clearing price of FM capacity trough at 13:00-14:00. 14:00 there was a trough, and FM capacity clearing prices all rose and fell steadily within the specified range. The FM mileage clearing price is basically stable at around RMB 15/MWh, which determines the FM mileage revenue of each market participant and is also affected by the market FM demand.

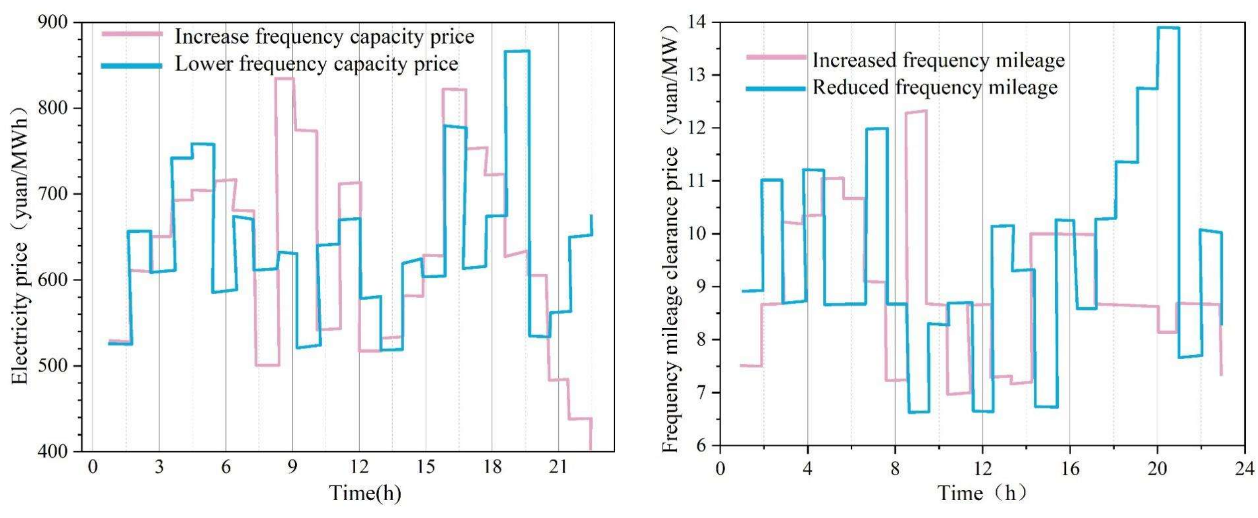

(a)FM capacity clearance price

(b)The frequency range is cleared for price

Fig. 7. FM auxiliary service market clearing price

6. Conclusion

In this paper, blockchain technology and fuzzy neural network are introduced to construct a short-term power load forecasting model. After that, a two-stage stochastic method is used to construct a decision-making model for virtual power plants to participate in spot market transactions. The main conclusions are as follows:

1) The virtual power plant market trading model based on fuzzy logic has better prediction results for the whole day's electricity load, which obviously improves the accuracy and stability of load prediction, and its average absolute error of prediction (1.095%) is reduced by 2.925% compared with the traditional BP algorithm model.

2) In the moment of great wind and light, the virtual power plant can get more chances of winning the bidding in the electric energy market with a lower offer price. In addition, by aggregating high-quality FM resources such as energy storage, the virtual power plant can improve the comprehensive FM performance and be very competitive in the FM market. Considering the fluctuation of wind power and photovoltaic output, the bidding capacity of virtual power plants in the electric energy market and the FM market is reasonably allocated, and the bidding scheme of virtual power plants is derived under the premise of taking into account the riskiness and profitability.

Funding

The Technology Project of the Guangdong Power Exchange Center (Project No.: GDKJXM20231634).

References

[1] Saboori, H., Mohammadi, M., & Taghe, R. (2011, March). Virtual power plant (VPP), definition, concept, components and types. In 2011 Asia-Pacific power and energy engineering conference (pp. 1-4). IEEE.

[2] Giuntoli, M., & Poli, D. (2013). Optimized thermal and electrical scheduling of a large scale virtual power plant in the presence of energy storages. IEEE Transactions on Smart Grid, 4(2), 942-955.

[3] Rahimiyan, M., & Baringo, L. (2019). Real-time energy management of a smart virtual power plant. IET Generation, Transmission & Distribution, 13(11), 2015-2023.

[4] Shabanzadeh, M., Sheikh-El-Eslami, M. K., & Haghifam, M. R. (2017). An interactive cooperation model for neighboring virtual power plants. Applied energy, 200, 273-289.

[5] Baringo, L., Rahimiyan, M., Baringo, L., & Rahimiyan, M. (2020). Virtual power plants. Virtual Power Plants and Electricity Markets: Decision Making Under Uncertainty, 1-7.

[6] Zhong, W., Murad, M. A. A., Liu, M., & Milano, F. (2020). Impact of virtual power plants on power system short-term transient response. Electric Power Systems Research, 189, 106609.

[7] Mao, T., Guo, X., Xie, P., Zhou, J., Zhou, B., Han, S., ... & Sun, L. (2020, November). Virtual power plant platforms and their applications in practice: a brief review. In 2020 IEEE Sustainable Power and Energy Conference (iSPEC) (pp. 2071-2076). IEEE.

[8] Guo, W., Liu, P., & Shu, X. (2021). Optimal dispatching of electric-thermal interconnected virtual power plant considering market trading mechanism. Journal of Cleaner Production, 279, 123446.

[9] Yu, Z., Qiu, Z., Cai, Y., Tao, W., Ai, Q., & Wang, D. (2023). Hybrid Game Trading Mechanism for Virtual Power Plant Based on Main-Side Consortium Blockchains. Electronics, 12(20), 4269.

[10] Liu, X. (2022). Research on bidding strategy of virtual power plant considering carbon-electricity integrated market mechanism. International Journal of Electrical Power & Energy Systems, 137, 107891.

[11] Yin, S., Ai, Q., Li, J., Li, D., & Guo, Q. (2022). Trading mode design for a virtual power plant based on main-side consortium blockchains. Applied Energy, 325, 119932.

[12] Liu, D., Xiao, F., Wu, J., Ji, X., Xiong, P., Zhang, M., & Kang, Y. (2023). Electricity-Carbon Joint Trading of Virtual Power Plant with Carbon Capture System. International Transactions on Electrical Energy Systems, 2023(1), 6864403.

[13] Lyu, X., Xu, Z., Wang, N., Fu, M., & Xu, W. (2019). A two-layer interactive mechanism for peer-to-peer energy

trading among virtual power plants. Energies, 12(19), 3628.

[14] Seven, S., Yao, G., Soran, A., Onen, A., & Muyeen, S. M. (2020). Peer-to-peer energy trading in virtual power plant based on blockchain smart contracts. Ieee Access, 8, 175713-175726.

[15] Yang, D., He, S., Chen, Q., Li, D., & Pandžić, H. (2019). Bidding strategy of a virtual power plant considering carbon-electricity trading. CSEE Journal of Power and Energy Systems, 5(3), 306-314.

[16] Cao, J., Yang, D., & Dehghanian, P. (2024). Cooperative operation for multiple virtual power plants considering energy-carbon trading: A Nash bargaining model. Energy, 307, 132813.

[17] Feng, Y., Jia, H., Wang, X., Ning, B., Liu, Z., & Liu, D. (2023). Review of operations for multi-energy coupled virtual power plants participating in electricity market. Energy Reports, 9, 992-999.

[18] Geng, J., Yu, S., Chen, A., Wang, H., Yan, B., Li, L., ... & Wang, Q. (2022). Evidence Mechanism of Power Dispatching Instruction Based on Blockchain. Computer Systems Science & Engineering, 43(2).

[19] Ruxia Yang,Hongchao Gao,Fangyuan Si & Jun Wang. (2024). Intelligent Scene-Adaptive Desensitization: A Machine Learning Approach for Dynamic Data Privacy in Virtual Power Plants. Electronics(6),

[20] Jinghao Chen,Lingyun You,Ting Du,Jian Xiao,Yongjia Cai,Pengyu Qu & Xiankun Ji. (2024). Damage constitutive model of RAC under triaxial compression based on weibull distribution function. Construction and Building Materials138499-138499.

[21] Gao Wen,Hei Xinhong & Wang Yichuan. (2023). The Data Privacy Protection Method for Hyperledger Fabric Based on Trustzone. Mathematics(6),1357-1357.

[22] Zhaoyang Liu,Yuteng Xiao,Honglei Wang,Chunyan Li & Hongsheng Yin. (2024). BBM: A novel beta-binomial-distribution-based biclustering algorithm for mining m6A co-methylation patterns. Expert Systems With Applications125121-125121.